APPENDIX: CALCULATION OF INTERPHASE CONCENTRATIONS WITH LANGMUIR ISOTHERM

If the Langmuir isotherm expression is used to describe the equilibrium relationship, Eq. 9 is given as

$$q_{s_i} = \frac{a_i c_{s_i}}{1 + \sum_{j=1}^{N} b_{i_j} c_{s_j}} \tag{A1}$$

where a_i and b_i are the Langmuir adsorption parameters for the single i-th species. Eq. A1 can be rewritten as

$$q_{s_i} = \frac{a_i c_{s_i}}{D} \tag{A2}$$

and

$$D = 1 + \sum_{j=1}^{N} b_j c_{s_j} \tag{A3}$$

Substituting Eq. A2 into Eq. 8b, one has

$$c_{s_i} \frac{a_i}{D} = \phi_i (c_i - c_{s_i}) + q_i \tag{A4}$$

Upon rearrangement, the above equation becomes

$$c_{s_i} = \frac{c_i + \dfrac{q_i}{\phi_i}}{1 + \dfrac{a_i}{\phi_i D}} \tag{A5}$$

Substituting Eq. A5 into Eq. A3, one has

$$D = 1 + \sum_{j=1}^{N} b_j \frac{c_j + \dfrac{q_j}{\phi_j}}{1 + \dfrac{a_j}{\phi_j D}} \tag{A6}$$

or

$$1 - D + \sum_{j=1}^{N} b_j \frac{c_j + \dfrac{q_j}{\phi_j}}{D + \dfrac{a_j}{\phi_j}} = 0 \tag{A7}$$

Thus, at point (l, m), with c_i and q_i known, the value of D can be obtained from Eq. A7. Once D is known, one can calculate c_{s_i} from Eq. A5 and q_{s_i} from Eq. A2.

Manuscript received November 14, 1980; revision received August 5, and accepted August 24, 1981.

Nitrogen Pollutant Formation in a Pulverized Coal Combustor: Effect of Secondary Stream Swirl

Concentrations of NO, NH_3, and HCN, together with coal particle burnout and gas composition, were measured during combustion of a bituminous coal. Control of incoming secondary gas swirl level and overall stoichiometric ratio led to significant reductions in nitrogen oxide pollutant concentration. In-situ measurements showed that coal particles were confined near the reactor center during rapid particle reaction. This took place in a locally fuel-rich environment, producing near-quantitative conversion of fuel-nitrogen to NH_3 and HCN, with some NO. Subsequent gas phase reactions of these nitrogen species were identified as important in establishing the ultimate NO concentration.

N. S. HARDING, JR.,
L. D. SMOOT and
P. O. HEDMAN

Chemical Engineering Department
Brigham Young University
Provo, UT

SCOPE

It has been shown (e.g., Pershing et al., 1975; Rees et al., 1980) that control of nitrogen oxide can be achieved through control of the pulverized coal mixing and combustion processes. It has also been shown (Pershing and Wendt, 1979) that oxidation of the nitrogen in the coal is the major source of the oxides of nitrogen, and that NO can be controlled through staging (Chen et al., 1980; Wendt, 1980). However, work is continuing to understand the NO formation and to further reduce NO levels. The objective of this work was to investigate the extent and causes of NO formation in the presence of secondary inlet air swirl level. Experiments were conducted in a cylindrical, laboratory pulverized coal combustor (13.7 kg coal/h) with samples being withdrawn 145 cm aft of the fuel-inlet port. Pulverized coal and air were injected through a cylindrical primary port while the secondary air stream was injected in a swirling fashion surrounding the primary stream. Measurements were made on gas composition (Ar, CO, CO_2, CH_4, H_2, N_2, O_2), elemental particulate composition (ash, C, H, N), and pollutant concentration (NO, NH_3, HCN). Effects of secondary stream swirl, stoichiometric ratio, primary stream velocity and solids loading level, coal particle size, and secondary stream preheat temperature were tested on coal burnout and N-pollutant level.

Experiments were also conducted at three swirl levels with gas-particulate samples obtained at various axial and radial positions. Resultant data provided NO concentration maps for interpreting the test results.

N. S. Harding, Jr., is currently with Conoco, Inc., Library, PA.

0001-1541-82-7939-0573-$2.00.

CONCLUSIONS AND SIGNIFICANCE

Stoichiometric ratio (*SR*) and secondary swirl (*S*) significantly influenced N-pollutant concentrations. An 88% reduction in NO was obtained while operating fuel-rich (*SR* = 0.66) at high secondary swirl compared to fuel-lean operation (*SR* = 1.32) without a swirling secondary stream. A reduction in NO by a factor of nearly 4 was obtained through use of the lower *SR* value, while an additional factor of 2 was obtained through use of secondary swirl (Figure 2). Variation in primary stream velocity, secondary air temperature, solids loading, and coal size had only a small impact on coal burnout and NO concentration.

NO concentration maps showed dramatic changes in the location of maximum NO concentration as the secondary stream swirl number was increased. Results suggest near-quantitative conversion (>80%) of nitrogen to NO and particularly NH_3 and HCN in the upper regions of the combustor.

Application of the Fenimore (1976, 1979) fuel-rich gaseous flame mechanism for NO formation to coal dust flames suggests that gas phase reactions of nitrogen intermediates to NO and with NO to N_2 are important rate controlling steps in NO formation in pulverized coal flames.

INTRODUCTION

During the coal combustion process, nitrogen oxides (NO_x) arise from one of two processes, either thermal fixation of atmospheric nitrogen or by reactions involving fuel nitrogen during coal devolatilization and char oxidation. NO_x formation processes are reviewed in detail by Malte and Rees (1979). From the work of several investigators (e.g., Pershing et al., 1975; Song et al., 1977; Pohl and Sarofim, 1977; Pershing and Wendt, 1979; and Snow et al., 1979), the relative amounts of NO_x from each of the previously mentioned sources are approximately as follows: Thermal nitrogen, 10–20% NO_x; fuel nitrogen during devolatilization, 50–70% NO_x and during char oxidation, 20–30% NO_x.

While swirl has been widely used as a means of stabilizing high intensity flames (Syred et al., 1971; Beer and Chigier, 1972; Lilly, 1977), it has only recently been applied to pollutant control. The swirl number S, has been used as a parameter to describe flow patterns where a tangential motion is given to the incoming feed streams (Syred and Beer, 1974). The swirl number is defined as the ratio of the axial flux of angular momentum divided by the axial flux of axial momentum times the burner (i.e., coal injector) radius. Beer and Chigier (1972) have shown that for swirl burners with moveable-block swirl generators, the theoretical secondary stream swirl number for a non-swirling primary stream flow is:

$$S_s^t = (\sigma A / 2\pi B R_b) \qquad (1)$$

A more detailed description of the swirl generator, the derivation of Eq. 1, and the calibration of the swirl generator are given in Harding (1980).

EXPERIMENTAL FACILITY AND TEST PROGRAM

The coal combustor of Figure 1 has been described in detail elsewhere (Thurgood, et al., 1980). The burner includes a moveable-block swirl generator to provide tangential motion to the secondary air stream. This type of swirl-burner has been commonly used (Beer and Chigier, 1972) to simulate a single burner of a large utility boiler. However, large utility burners often have several individually adjustable swirl vanes. Only a portion of the secondary air passes through these vanes, and as a result the flames are long. All of the secondary air passes through the swirl blocks of the laboratory burner, giving more control and a shorter flame.

This work emphasizes the details of the earliest regions of combustion, since the particle residence time through the combustor was only less than 300 msec. A majority of the coal was burned (⩾80%) and the nitrogen-containing pollutants have formed to significant levels in this region.

An L-shaped, water-quenched probe was used for all samples near the combustor outlet (145 cm) while a special rotatable probe for swirling flows was used while sampling in the higher regions of the combustor, where swirling of the flow was significant. Attempts were made to sample as near to isokinetic conditions as possible by balancing the internal probe pressure with the static wall pressure at the same axial location. This method has neglected effects of radial pressure gradient that exist in regions of strongly swirling flow.

The probe samples were separated into gas, liquid, and solid phases and each analyzed (Harding, 1980). The analyzed gases included Ar, H_2, O_2, N_2, CO, CO_2, CH_4, and NO; the liquid from the quench water was analyzed for HCN and NH_3 (Price, 1980). Weight fractions of ash, nitrogen, carbon and hydrogen were determined for the particulate samples.

The coal (Utah, high-volatile B, bituminous) was pulverized to 70% less than 200 mesh with a resultant mass mean particle di-

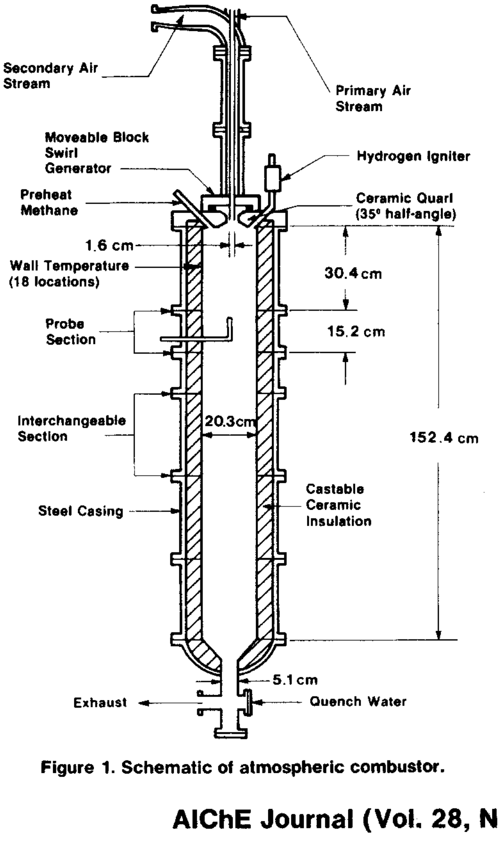

Figure 1. Schematic of atmospheric combustor.

TABLE I. TEST CONDITIONS AND VARIABLES

I. Test Series 1 (Effects of Variables) Variables	Values
Part A (18 Tests)	
Stoichiometric Ratio, *SR*	1.32, 1.00, 0.66
Secondary Swirl Number, S_s^e	0.0, 1.4, 3.4
Primary Velocity, m/s	30.5, 15.2
Part B (8 Tests)	
Stoichiometric Ratio, *SR*	1.32, 1.00
Particle Size, µm	50, 14
Secondary Temperature, K	589, 478
Part C (4 Tests)	
Solids Loading, wt.%	40, 60
Stoichiometric Ratio, *SR*	1.32, 1.00
II. Test Series 2 (Profiles)	
Secondary Swirl Number, S_s^e	0, 1.4, 3.4
Primary Air Feed Rate, g/s	5.8
Primary Argon Feed Rate, g/s	0.3
Coal Feed Rate, g/s	3.8
Mean Particle Diameter, µm	49.9
Solids Loading, wt. %	40.0
Primary Velocity, m/s	30.5
Secondary Air Feed Rate, g/s	29.9
Overall Stoichiometric Ratio	1.0
Primary Preheat Temperature, K	356
Secondary Preheat Temperature, K	589

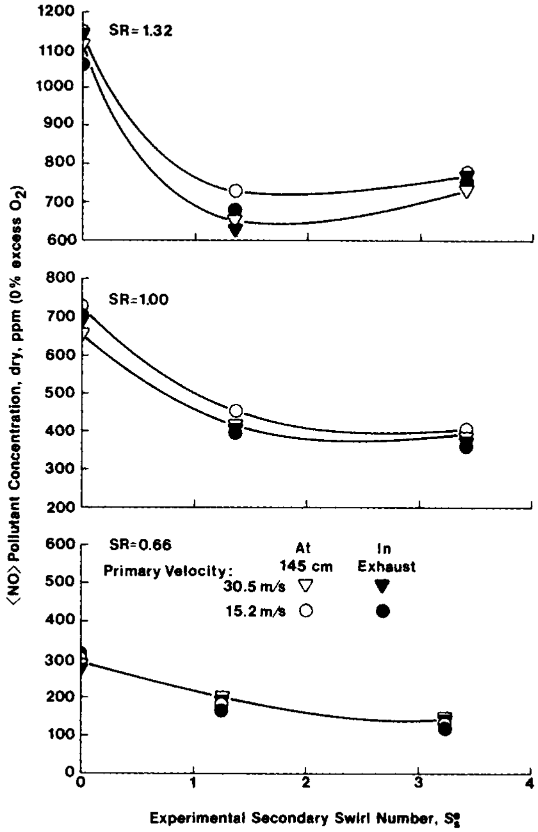

Figure 2. Effect of swirl no., stoichiometric ratio, and primary stream velocity on ⟨NO⟩ pollutant concentration; test series 1.

ameter of 49.9 µm. The coal contained approximately 2.4% moisture, 45.4% proximate volatiles, 43.7% fixed carbon, and 8.6% ash. Its elemental composition was 69.8% carbon, 5.6% hydrogen, 1.4% nitrogen, 0.5% sulfur, and 13.2% oxygen by weight, plus ash.

In the first set of tests, primary velocity, primary solids loading, coal particle size, secondary preheat temperature, secondary swirl number, and stoichiometric ratio were varied. Table 1 lists the range of variables studied. Other test conditions common to all tests were coal feed rate of 13.7 kg/hr and a primary temperature of 356 K. The objective of this test series was to determine the burner parameters which would result in minimum levels of nitrogen pollutant concentration at the combustor exit, with acceptable levels of coal burnout (i.e., >80%).

The second part of the test program involved detailed mapping of the combustor with test conditions determined from part 1 (Table 1). The objective of this second set of tests was to determine causes for the observed effects of swirl and to provide data for comparison with model predictions (Smith and Smoot, 1980).

Material balances were performed to verify accuracy and reliability of the tests. Argon, oxygen, hydrogen, ash, and carbon balances made during part 1 were better than the balances resulting from profile measurements based on samples from near-entrance regions in the combustor. The average error from the independent oxygen balance for all but three tests in both test series was ±19.4%. Errors in the near-entrance regions resulted from significant gradients in velocity, pressure and concentration, and from the problems caused by the swirling motion of the fluid.

RESULTS AND DISCUSSION

Test Series 1: Effects of Variables

To improve data reliability, several gas-particle samples were obtained at the near-exit station (145 cm) and in the gas exhaust line. The five radial samples were integrated to give a mass-averaged value (i.e., ⟨NO⟩) for each test.

Figure 2 is a summary of the effects of secondary swirl number, stoichiometric ratio and primary velocity on the NO concentration. The decrease in primary velocity from 30.5 to 15.2 m/s had only a slight effect on NO concentration. A substantial decrease in the NO level was observed as SR was decreased from 1.32 to 0.66. This is a well-documented finding (e.g., Heap et al., 1972; Pershing et al., 1975; Chen et al., 1980; Rees et al., 1980) and is related to the decrease in oxygen available to react with fuel-nitrogen species.

Also from Figure 2, a large decrease in NO was observed when increasing S_s^e from 0 to 1.4 at *SR* of 1.32 and 1.0. A small increase in NO was observed at an *SR* = 1.32 when the swirl number was further increased to a value of 3.4. At a stoichiometric ratio of 1.0, a small decrease in NO was observed between the middle and high swirl numbers, while at *SR* = 0.66, a continual decrease in NO was observed as the swirl number was increased. The decrease, followed by an increase in NO with increasing swirl number, is probably caused by the effects of mixing. With no swirl, the flame is stabilized toward the middle of the combustor, providing time for significant mixing of air and the coal before the onset of combustion. This condition gave the maximum NO levels measured. As secondary swirl number was increased, the flame attached to the burner, promoting coal reaction in the fuel-rich region prior to significant particle dispersion or gas mixing. As the swirl was increased beyond those values where the minimum NO levels were observed, the mixing of air and fuel was apparently enhanced, resulting in higher NO values.

With the additional measurements made for HCN, NH_3, and char nitrogen, it was possible to calculate fractional amounts of NO, NH_3, and HCN formed from the coal nitrogen released. Four key assumptions were used in this analysis. First, it was assumed that the sample gases from coal reactions came from the char particles in that sample. This is a good assumption near the exit of the combustor where nearly complete mixing of the gas and particles had occurred, since samples drawn from each radial location would be similar. Also, it was assumed that carbon from the coal shows up in the gas phase as either CO, CO_2, CH_4, or C_2H_6, neglecting soot formation. Further, it was assumed that NO from thermal fixation of the atmospheric nitrogen (Zeldovich, 1946) and NO formed from "prompt NO" (Fenimore, 1971; Hayhurst and Vince, 1980) was small. Finally, negligible formation of other N-containing species (e.g., NO_2) was assumed.

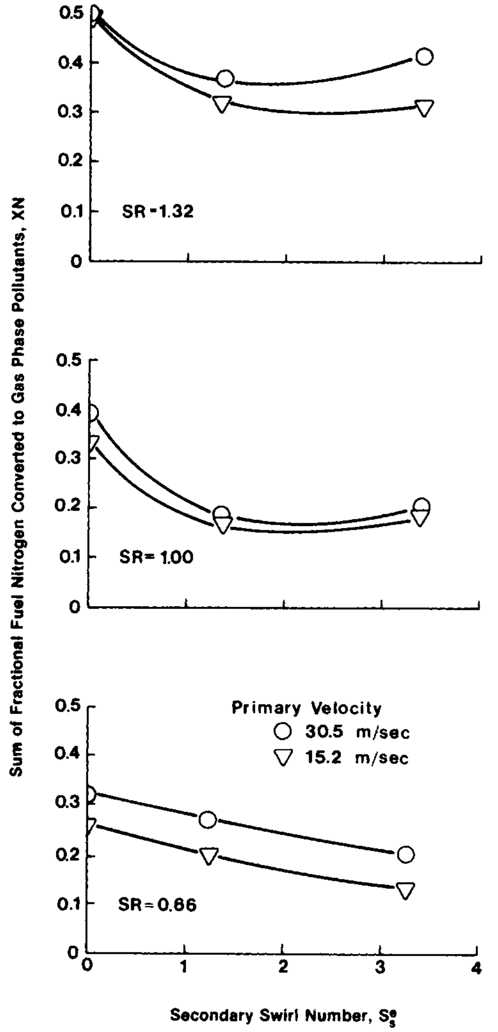

Figure 3. Effect of swirl no., stoichiometric ratio, and primary stream velocity on fractional fuel nitrogen converted to gas phase pollutants; test series 1.

The fraction of each of the nitrogen-containing species was determined, assuming that all nitrogen from the coal was contained in NO, HCN, NH_3, char nitrogen, or N_2. The total gaseous nitrogen pollutant species fraction (XN = NO + NH_3 + HCN) was calculated, as shown in Figure 3. Lowering SR from 1.32 to 1.0 causes a decrease in fractional conversion of total nitrogen pollutant species. A much smaller decrease in XN is noticed between SR = 1.0 and SR = 0.66. This is due to the increase in HCN and NH_3 values measured at SR = 0.66.

Swirl had a major effect in overall reduction of these nitrogen pollutants at all three SR values. In fact, the trends of Figure 3 are very similar to those for NO (Figure 2). This is due primarily to the small amounts of HCN and NH_3 present at SR = 1.32 and 1.0. However, at the most fuel-rich condition (SR = 0.66), the swirl number required for maximum reduction of XN appears to be beyond the highest swirl number tested.

Variations in primary velocity had little effect on XN (Figure 3). XN values for a primary velocity of 15.2 m/s are generally lower than the corresponding values at 30.5 m/s. Since the primary stream momentum was decreased by a factor of two (the axial velocity was reduced by half), a central core should decay sooner in the swirling flame with the lower velocity. This would increase mixing of fuel and oxidizer and enhance oxidation of the HCN and NH_3.

The effects of primary solids loading, particle size, and secondary temperature were much less pronounced than were effects of stoichiometric ratio and swirl number. An increase in primary solids loading from 40 to 60 weight percent resulted in very little change in NO concentration measured near the combustor exit, but did result in a slight increase in XN, due to the increased formation of HCN and NH_3, especially in the central region of the combustor.

The burning of small particles ($\bar{d}_p$ = 13.7 μm) resulted in no apparent change in NO concentration measured at 145 cm, compared to results for larger particles ($\bar{d}_p$ = 49.9 μm). The decrease in secondary temperature from 589 K to 478 K caused a slight decrease in NO and a small increase in XN.

This first series of experiments provided several important observations. First, swirl of the secondary stream can be an effective method of reducing NO pollution levels. Second, combining high swirl and low SR values resulted in an order of magnitude decrease in NO concentrations compared to fuel-lean operation with S_s^e = 0. Finally, results show that measurements of total nitrogen pollutants (NO+HCN+NH_3) provide useful information for data interpretation.

Test Series 2: Profiles

Gas-particle samples were obtained throughout the combustor to explore causes of the observed NO reduction with increasing swirl and to evaluate detailed coal flame models.

Figure 4 shows the effects of secondary stream swirl on the major gas species and NO measured at axial positions of 25.4 and 109.2 cm. The radial profiles at 25.4 cm (Figure 4a) show increasing NO and CO_2 values from the centerline to peak values about two centimeters off centerline. O_2 concentration shows opposite trends. CO concentrations peak at the centerline and decline to near zero at five cm. At 109 cm (Figure 4b), profiles are quite flat. From these and other data (Harding, 1980), there appears to be a fuel-rich core in the upper-center of the combustor surrounded by a reaction zone about 2–3 cm thick. Radial profiles of particle mass flux (Harding, 1980) showed steep particle mass flux gradients in the upper regions of the combustor, confirming a fuel-rich, coal dust core.

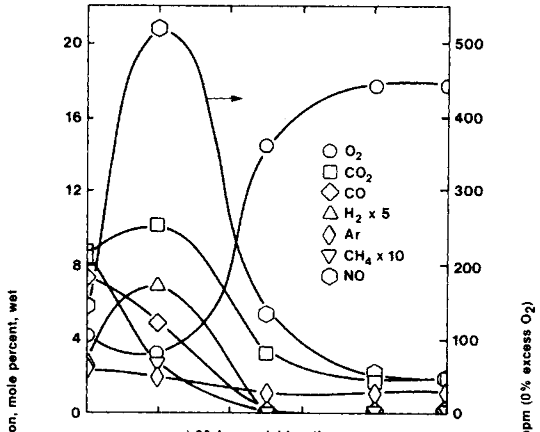

a) 25.4 cm axial location

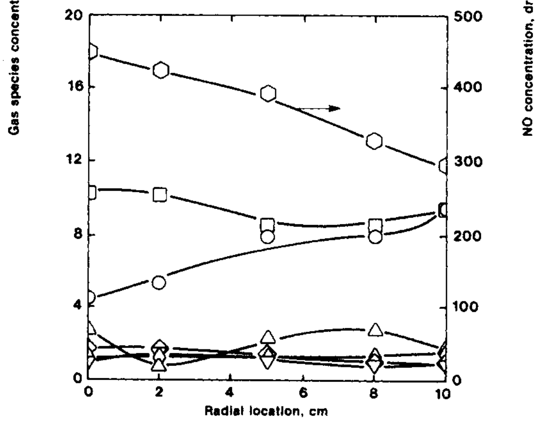

b) 109.2 cm axial location

Figure 4. Radial species profiles at S_s^e = 1.4.

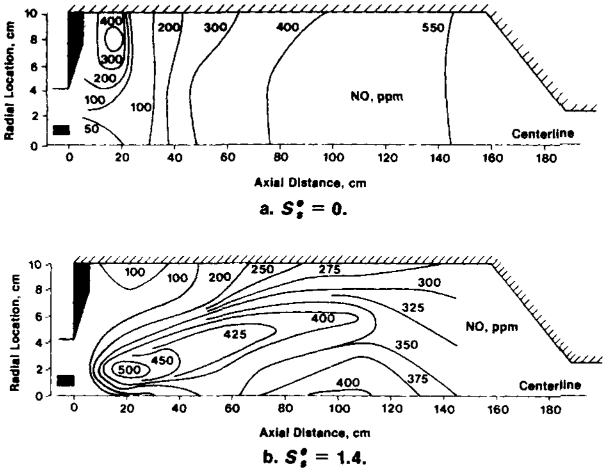

a. $S_s^e = 0$.

b. $S_s^e = 1.4$.

Figure 5. Combustor profiles for NO, with *SR* = 1.0 (ppm, as measured).

From these and other radial profiles, concentration maps of NO were prepared (Figure 5). The large decrease in NO with increased swirl can be explained by comparing the NO map for zero swirl (Figure 5a) to that for a swirl number of 1.4 (Figure 5b). The flame was not attached at the burner in the case of $S_s^e = 0$; in fact, the onset of combustion was 30–40 cm from the burner, where NO began forming (Figure 5a). The NO level increased steadily as the coal burned, giving the highest NO concentration near the exit of the combustor.

At $S_s^e = 1.4$, the flame was attached to the burner and the maximum NO values were located in a small region near the centerline and about 20 cm from the burner (Figure 5b). The large recirculation region at the top of the reactor shown for zero swirl is much closer to the wall with much lower NO levels in the case with swirl. Temperature profiles from measurements with a single-shield, suction pyrometer were also made and are very similar in shape to the NO concentration maps shown in Figure 5 (Harding, 1980).

In order to resolve the fate of the fuel nitrogen, integrated axial flow rates of HCN, NH_3, and NO were calculated at each axial location for $S_s^e = 1.4$. The amounts of nitrogen in the various gaseous pollutants and the char were determined, and the fraction of fuel nitrogen showing up as NO, HCN, or NH_3, was calculated, neglecting thermal NO formation.

Figure 6 shows these data for the regions aft of 40 cm. NH_3 and HCN have formed in the forward regions of the reactor and predominate as the major pollutant species. The NO level is less than half the magnitude of HCN or NH_3. At about 70 cm axially, the fraction of fuel nitrogen as HCN and NH_3 has decreased significantly without a large increase in the fraction of nitrogen converted to NO. In the aft regions, significant amounts (~70%) of N_2 have apparently formed from subsequent reactions of HCN and NH_3.

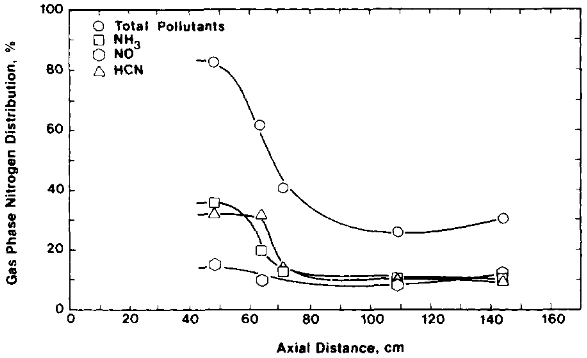

6. Effect of axial location on distribution of gas phase fuel nitrogen (radially integrated values), $S_s^e = 1.4$, *SR* = 1.0.

These results suggest near-quantitative (>80%) conversion of gaseous fuel nitrogen into NO + HCN + NH_3 (i.e., *XN*) in the upper regions. This observation has been observed in gas-phase flames doped with a fuel-nitrogen containing gas (Corlett et al., 1979; Song et al., 1980). If this observation is valid in coal dust flames, then interpretation and modeling of NO formation can be greatly simplified, since the local concentration of HCN and NH_3 can be determined from coal devolatilization rates.

Gas and Particle Mixing Rates

Centerline gas concentration and particle mass flux characterize mixing rates of gas and particles, respectively. The gas mixture fraction, f_g, is defined as:

$$f_g = m_{pg}/(m_{pg} + m_{sg}) \tag{2}$$

From argon and nitrogen balances, the local gas mixture fraction has been determined throughout the combustor. The gas mixture fraction represents a measure of the extent of mixing between primary and secondary gas streams at a given point in the reactor.

In a similar manner, a particle mixture fraction is defined by:

$$f_k = m_{kp}/(m_{kp} + m_{kg} + m_{gp} + m_{gs}) \tag{3}$$

This parameter varies with both the extent of mixing and of particle reaction, because the mass of coal collected is related both to the dispersion of the coal and its extent of reaction. Thurgood (1979) describes the procedure for determining f_g and f_k.

Figure 7 shows centerline gas and particle mixture fractions for a secondary swirl number of 1.4. These values are plotted in a logarithmic method that normalizes the mixture fraction (Leavitt, 1980). Also shown is the normalized gas mixture fraction (F_g) from Thurgood et al. (1980) for tests with parallel injection of primary and secondary streams, i.e. $S_s^e = 0$. The mass flow rates of primary and secondary air used by Thurgood with this same combustor were similar to those in this study. From Figure 7, the gas mixing rate for $S_s^e = 1.4$ appears to be comparable to that determined for $S_s^e = 0$. Data scatter preclude firm conclusions. The data also suggest that particles are not yet well mixed at the reactor exit, and that particle dispersion is not rapid in upper regions.

From the profile and mixing data presented, the swirling secondary stream appears to have reduced the NO concentration by creating a central, fuel-rich particle core which is confined within a surrounding flame. The swirling fluid has apparently caused sufficient mixing to permit the flame to attach to the burner. The radiation from the flame to the central core causes the nitrogen to evolve in a fuel-rich environment, thus creating high levels of HCN and NH_3. As gas mixing continues, intermediate species react to form molecular nitrogen and smaller quantities of NO.

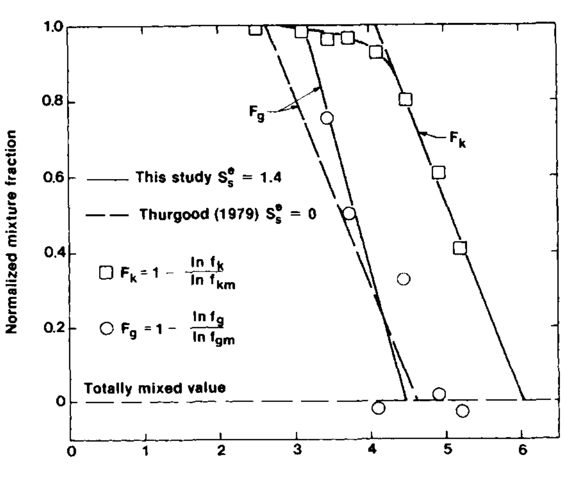

Figure 7. Effect of axial location on extent of gas mixing and particle dispersion.

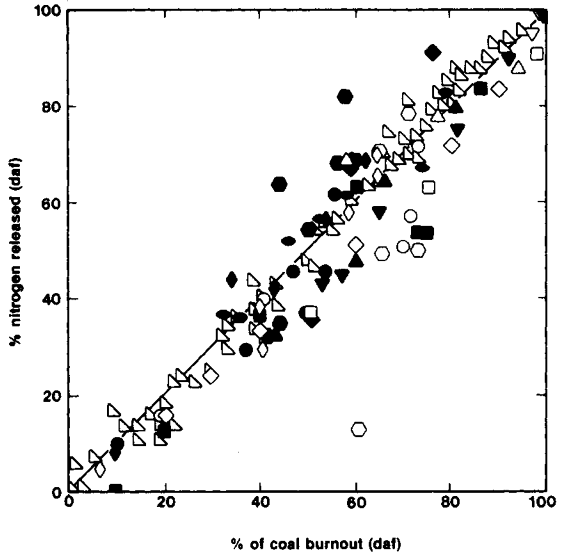

Figure 8. Effect of percent coal burnout (daf) on percent nitrogen released. ● Ohio #2 (Solomon & Colket, 1978) ○ Lower Kitt (Solomon & Colket, 1978) ▼ Mont. Lignite, 1,250 K (Song et al., 1977) ▽ Mont. Lignite, 1,750 K (Song et al., 1977) ● Bituminous (Rees et al., 1980) ▲ Mont. Lig. Char, 1,250 K (Song et al., 1977) △ Mont. Lig. Char, 1,750 K (Song et al., 1977) ■ Bit. & Lig. (Pohl & Sarofim, 1977) □ Char (Pohl & Sarofim, 1977) ○ Wyodak (Blair et al., 1977) ◇ Bituminous (Rees et al., 1980) ● Arkwright (Blair et al., 1977) ● Ill. #6 (Blair et al., 1977) ◇ Bit. (Thurgood, 1979) ● Bit. (Skinner, 1980) △ Bit. (this study).

NO FORMATION PROCESSES

The formation of NO during coal combustion is divided into four parts: 1) char nitrogen release, 2) formation of nitrogen intermediates, 3) competing NO and N_2 formation rates, and 4) NO decay. Nitrogen evolves from the coal at approximately the same rate as the coal reacts, as illustrated in Figure 8 for results of 10 different coals from eight investigations, including data from this study. Coal devolatilization time is of the order of 5–100 msec (Kobayashi et al., 1977) with a much longer time (>500 ms) usually required for char oxidation (Smoot, 1980). Predictable rates of devolatilization of coal (Kobayashi et al., 1977) and results of Fig. 8, provide an estimate of the rate of fuel nitrogen emission.

The results of Fig. 6 suggest that fuel nitrogen in the gas phase may be quantitatively converted to NO, HCN, and NH_3 with NH_3 and HCN clearly dominating as the major pollutant species in the upper regions. Fenimore (1976, 1979), proposed a mechanism for prediction of NO levels in fuel-rich, nitrogen-doped, gaseous flames. The nitrogen-containing species were assumed to react rapidly to nitrogenous-intermediates (NI), which react with oxidants (Ox) to form NO at a rate, R_1,

$$NI + Ox \xrightarrow{k_1\ \mathrm{NO}\ +\ \ldots} \qquad (4)$$

while the same or similar intermediates also destroy NO, forming N_2 at a rate, R_2:

$$NI + NO \xrightarrow{k_2\ \mathrm{N_2}\ +\ \ldots} \qquad (5)$$

Assuming that the same intermediate is involved in both reactions, the following expression was obtained by combination of Eqs. 4 and 5 and integration over a region in the combustor (Fenimore, 1976):

$$2\alpha\, ln \left[\frac{\alpha - [\mathrm{NO}]_o}{\alpha - [\mathrm{NO}]_i}\right] = -([RN]_i - [RN]_o + [\mathrm{NO}]_o - [\mathrm{NO}]_i) \qquad (6)$$

where $\alpha = k_1\,[\mathrm{NO}]/R_2 = k_1\,[\mathrm{Ox}]/k_2$. From the inlet concentrations of fuel nitrogen not yet converted to NO or N_2, the outlet concentration of NO can be estimated if a value for α is known. An attempt was initially made to use the α correlation of Fenimore (1979) directly, i.e., $\alpha = 700\,[\mathrm{H_2O}]\exp(-25{,}200/T)$. Predicted exit NO values were generally within a factor of two, but computed results for inside the reactor were generally much worse.

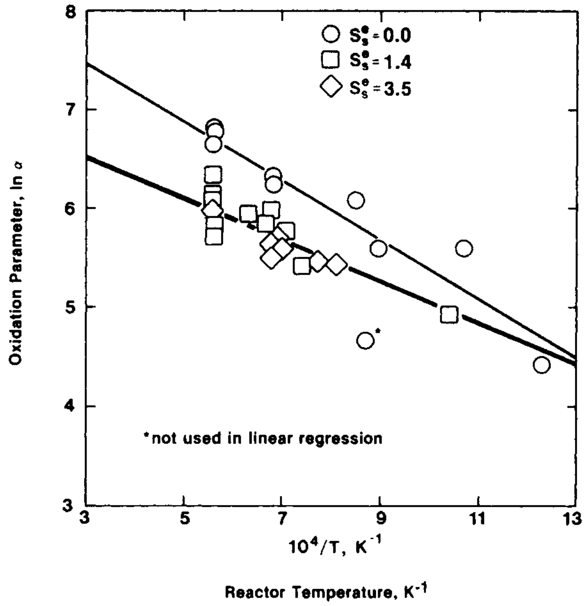

Figure 9. Correlation of oxidation parameter, α, with reactor temperature and swirl level.

Subsequently, a separate correlation for α was established for the pulverized coal diffusion flame as shown in Figure 9. The temperatures used in the upper regions were measured temperatures while the temperatures used in the exit regions of the combustor were predicted with a one-dimensional combustion model (Smith and Smoot, 1980). The data of Figure 9 appear to fall into two groups: one without swirl and one with swirl. The activation energy for both groups is in the range of 5 kcal/mol, which is significantly different from the Fenimore value.

The α correlation of Figure 9, together with NH_3 and char-N concentrations measured in the combustor, were used in Eq. 6 to estimate the NO concentration for tests in this study (Figure 10). While these results are encouraging, significant variations in local temperature that were not considered suggest caution in use of the correlation.

Fenimore (1976) further postulated that fuel nitrogen in the gas

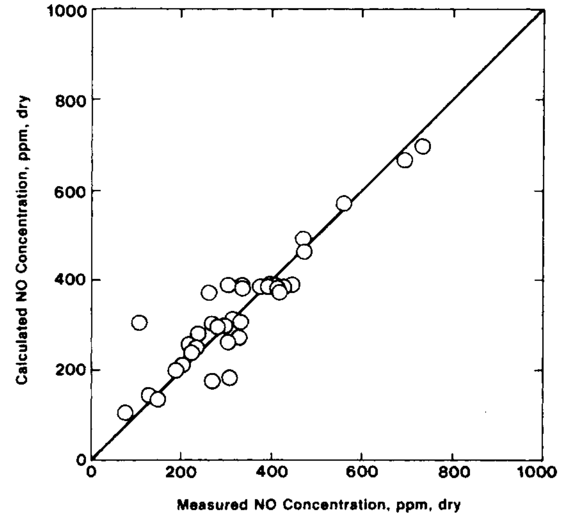

Figure 10. Comparison of calculated and measured NO concentrations.

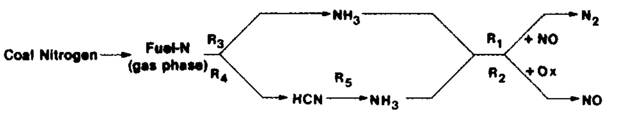

Figure 11. Mechanism of NO and N_2 formation in pulverized coal combustion systems (major features from Fenimore, 1976).

phase reacts very rapidly to form intermediate nitrogen species (NI) such as ammonia and cyanide. The intermediate N-species react more slowly (rate-controlling) with oxidant species to form either NO or with NO to form N_2, as illustrated in Figure 11. Based on the observations of Figure 6, it appears that R_4 is approximately equal to $R_3 + R_5$, since the concentration of HCN is about equal to that of NH_3, and the NO level is low. A parallel reaction scheme is reasonable, since HCN and NH_3 have about the same concentration. The NO level appears constant in the earlier regions, suggesting that $R_3 + R_5$ is of the same magnitude as $R_1 + R_2$. This is also substantiated by the apparent plateau of fuel nitrogen converted to NH_3 and HCN.

The more rapid decay of NH_3 compared to HCN suggests a series of reactions of HCN to NH_3 before a conversion to NO or N_2 takes place. However, the decrease in NH_3 and HCN is not followed by an increase in NO. This suggests that $R_1 \geqslant R_2$; thus, as soon as any NO is formed, it reacts rapidly with an ammonia derivative (NH_i) to form mostly N_2. The observation that R_1 appears to be greater than R_2 is supported by the fact that complete gas mixing has probably occurred by the end of the decline in HCN and NH_3 (Figure 7). The increase in oxidizer causes NO to be formed and to react with NH_i via R_3 or R_5 for form N_2.

ACKNOWLEDGMENTS

Financial support was received from the Electric Power Research Institute, Babcock and Wilcox, Foster Wheeler, IHI Heavy Industries (Japan) and Brigham Young University Research Division.

NOTATION

A = area burner (m^2)
B = thickness of swirl blocks (m)
daf = dry, ash free
$\bar{d}_p$ = mass mean particle diameter (μm)
F = normalized mixture fraction
f = mixture fraction
k = reaction rate constant (kmol, s, m)
m = sample mass (kg)
$[NI]$ = nitrogen intermediate (kmol m^{-3})
$[Ox]$ = oxygen concentration (kmol m^{-3})
ppm = parts per million by volume
R = reaction rate (kmol s^{-1})
r = primary jet radius (m)
R_b = burner radius (m)
RN = fuel-nitrogen not converted to N_2 or NO
S = swirl number
SR = stoichiometric ratio
T = temperature, K
XN = sum of HCN, NO, NH_3 (ppm)
z = axial distance from burner inlet (m)

Greek Letters

α = oxidation parameter (ppm)
σ = swirl block parameter

Subscripts/Superscripts

e = experimental
i = inlet
g = gas
k = particle
m = well-mixed value
o = outlet
p = primary
s = secondary
t = theoretical
1, . . . 5 = *reaction* 1, . . . 5

LITERATURE CITED

Beer, J. M., and N. A. Chigier, *Combustion Aerodynamics*, Applied Science Publishers, Inc., London (1972).

Blair, D. W., J. O. L. Wendt, and W. Bartok, "Evolution of Nitrogen and Other Species During Controlled Pyrolysis of Coal," *16th Symposium (International) on Combustion*, The Combustion Institute, Pittsburgh, PA, 475 (1977).

Chen, S. L., M. P. Heap, D. W. Pershing, R. K. Nihart, and D. P. Rees, "The Influence of Full Composition on the Formation and Control of NO_x in Pulverized Coal Flames," Western States Section Combustion Institute, Spring Meeting, Irvine, CA (1980).

Corlett, R. C., L. E. Monteith, and P. C. Malte, "Molecular Nitrogen Yields from Fuel-Nitrogen in Backmixed Combustion," *Combust. Sci. Tech.*, **19**, 95 (1979).

Fenimore, C. P., "Reactions of Fuel-Nitrogen in Rich Flame Gases," *Combust. and Flame*, **26**, 249 (1976).

Fenimore, C. P., "Studies of Fuel-Nitrogen Species in Rich Flame Gases," *17th Symposium (International) on Combustion*, The Combustion Institute, Pittsburgh, PA, 661 (1979).

Harding, N. S., "Effects of Secondary Swirl and Other Burner Parameters on Nitrogen Pollution Formation in a Pulverized-Coal Combustor," Ph.D. Dissertation, Brigham Young University, Provo, Utah (December, 1980).

Hayhurst, A. N., and I. M. Vince, "Nitric Oxide Formation from N_2 in Flames: The Importance of 'Prompt NO'," *Prog. Energy Combust. Sci.*, **6**, 35 (1980).

Heap, M. P., T. M. Lowes, and R. Walmsley, "The Effect of Burner Parameters on Nitric Oxide Formation in Natural Gas and Pulverized Fuel Flames," American Flame Days, American Flame Research Committee (1972).

Kobayashi, H., J. B. Howard, and A. F. Sarofim, "Coal Devolatilization at High Temperatures," *16th Symposium (International) on Combustion*, Combustion Institute, Pittsburgh, PA, 411 (1977).

Lilly, D. G., "Swirl Flows in Combustion: A Review," *AIAA J.*, **15**, 8 (1977).

Malte, P. C. and D. P. Rees, "Mechanisms and Kinetics of Pollutant Formation During Reaction of Pulverized Coal," p. 183–210, *Pulverized Coal Combustion and Gasification*, Smoot, L. D. and Pratt, D. T., eds., Plenum, NY (1979).

Pershing, D. W., G. B. Margin, and E. E. Berkau, "Influence of Design Variables on the Production of Thermal and Fuel NO from Residual Oil and Coal Combustion," *AIChE Symp. Ser.*, **71**, 148 (1975).

Pershing, D. W., and J. O. L. Wendt, "Relative Contributions of Volatile Nitrogen and Char Nitrogen to NO_x Emissions from Pulverized Coal Flames," *Ind. Eng. Chem. Process Des. Dev.*, **18**, 1 (1979).

Pohl, J. H., and A. F. Sarofim, "Devolatilization and Oxidation of Coal Nitrogen," *16th Symposium (International) on Combustion*, Combustion Institute, Pittsburgh, PA, 491 (1977).

Price, T. D., "Measurement of Pollutants in an Entrained-Flow Coal Gasifier," M.S. Thesis, Brigham Young University, Provo, Utah (1980).

Rees, D. P., L. D. Smoot, and P. O. Hedman, "Nitrogen Oxide Formation Inside a Laboratory Pulverized Coal Combustion," *18th Symposium (International) on Combustion*, Pittsburgh, PA, 1305 (1980).

Smith, P. J., and L. D. Smoot, "One-Dimensional Model for Pulverized Coal Combustion and Gasification," *Comb. Sci. Technol.*, **23**, 17 (1980).

Smoot, L. D., "Pulverized Coal Diffusion Flames: A Perspective Through Modeling," *18th Symposium (International) on Combustion*, Combustion Institute, Pittsburgh, PA, 1185 (1980).

Snow, G. C., W. L. Grosshandler, and P. C. Malte, "Measurement of Pollutant Species in Recirculative Coal Combustion," Western States Section, Combustion Institute, Spring Meeting, Provo, Utah (1979).

Solomon, P. R., and M. B. Colket, "Evolution of Fuel Nitrogen in Coal Devolatilization," *Fuel*, **57**, 749 (1978).

Song, Y. H., J. M. Beer, and A. F. Sarofim, "Fate of Fuel Nitrogen During Pyrolysis and Oxidation," 2nd Annual Symposium on Stationary Source Combustion, New Orleans, LA (1977).

Song, Y. H., D. W. Blair, V. J. Suminski, and W. Bartok, "Conversion of Fixed Nitrogen to N_2 in Rich Combustion," *18th Symposium (International) on Combustion*, Pittsburgh, PA, 53 (1980).
Syred, N., and J. M. Beer, "Combustion in Swirling Flows: A Review," *Combust. and Flame*, 23, 143 (1974).
Syred, N., N. A. Chigier, and J. M. Beer, "Flame Stabilization in Recirculation Zones of Jets with Swirl," *13th Symposium (International) on Combustion*, Combustion Institute, Pittsburgh, PA, 617 (1971).
Thurgood, J. R., L. D. Smoot, and P. O. Hedman, "Rate Measurements in a Laboratory-Scale Pulverized Coal Combustor," *Comb. Sci. and Tech.*, 21, 213 (1980).
Thurgood, J. R., "Mixing and Reaction Rate Resolution in Pulverized Coal Combustion," Ph.D. Dissertation, Brigham Young University, Provo, UT (1979).
Zeldovich, Y. A., "The Oxidation of Nitrogen in Combustion Explosions," *Acta Physiocochima*, 21, 577 (1946).

Manuscript received January 26, 1981; revision received August 31, and accepted September 16, 1981.

Statistical Estimation of Parameters in Vapor-Liquid Equilibrium

A new procedure for the estimation of parameters in two-component vapor-liquid equilibrium is presented. It allows for measurement errors in all variables and gives better fits than most other procedures because of the use of two relations between the variables rather than one as is commonly used. An approximate and an exact solution are described and the importance of using all thermodynamic and statistical information is illustrated for the Wilson and UNIQUAC models. New alternatives for analysis of residuals are also discussed.

HUGO PATINO-LEAL
and
P. M. REILLY
Department of Chemical Engineering
University of Waterloo
Waterloo, Ontario, Canada

SCOPE

The importance of phase equilibrium prediction in chemical process design has promoted the development of various semimechanistic models. An important aspect in the successful application of these models is the optimal estimation of their unknown parameters from limited experimental information. In this process of estimating parameters, it is important to use all the information that is available.

One source of information is the thermodynamics of the system. This supplies the equations relating the several variables. In the past, not all equations have been used; this work illustrates the improvement that can be achieved by using simultaneously all the equations involved.

Another problem with most previous attempts has been the use of estimation criteria which are basically arbitrary. Some of these assume some of the variables to be perfectly known. Our solution is a statistical one, based on the error-in-variables model (EVM), which gives optimal parameter estimation and allows for the presence of experimental error in all measured variables, giving general and flexible solutions, easy to apply.

Once the parameter estimates have been found, it is important to have an idea of how much uncertainty is involved in them, and how well the model represents the system. We present new alternatives for these aspects.

While the statistical principle of allowing for error in all measured variables is applicable to any formulation of the problem of describing vapor-liquid equilibria, we will illustrate its use as applied to the Wilson and UNIQUAC models. We will use the illustration further to show how our approach can be used to obtain residuals to assess the applicability of the mathematical model.

As a further objective of this paper, we intend to demonstrate the importance of using all the thermodynamic information which is available to supplement that provided by the experimental results.

CONCLUSIONS AND SIGNIFICANCE

Basic thermodynamics indicates that for a binary system to have two phases in equilibrium two equilibrium conditions must be satisfied simultaneously. We have found that these two relations provide important information, all of which should be used in order to estimate efficiently the parameters of the model.

The error-in-variables procedure presented here allows for the presence of experimental random error in all the variables involved. It also allows for more than one equilibrium condition to be satisfied and does not impose any restrictions on the form of the error covariance matrix. The exact solution presented is relatively simple to program, converges quickly and does not require the storage or inversion of large matrices. An alternative (approximate) solution is also presented which has proven to give very valuable results and involves a minimum of computation. The performance of these statistically sound techniques is remarkably better than methods based on arbitrary estimation criteria.

There are several ways in which one can check how well (or badly) a particular model is able to represent the data. We have been able to provide residuals to accomplish this check by an extension of standard statistical procedures.
